ARTICLE

Highly Efficient Synthesis of Clean Biofuels from Biomass Using FeCuZnAlK Catalyst

Song-bai Qiu[a], Yong Xu[a], Tong-qi Ye[a], Fei-yan Gong[a], Zhi Yang[a], Mitsuo Yamamoto[b], Yong Liu[c], Quan-xin Li[a*]

a. Department of Chemical Physics, Anhui Key Laboratory of Biomass Clean Energy, University of Science and Technology of China, Hefei 230026, China
b. College of Arts and Sciences, The University of Tokyo, 3-8-1 Komaba, Meguro-ku 153-8902, Japan
c. Hefei Tianyan Green Energy Development Co., Ltd., Hefei 230026, China

(Dated: Received on March 13, 2011; Accepted on May 13, 2011)

Highly efficient synthesis of clean biofuels using the bio-syngas obtained from biomass gasification was performed over $Fe_{1.5}Cu_1Zn_1Al_1K_{0.117}$ catalyst. The maximum biofuel yield from the bio-syngas reaches about 1.59 kg biofuels/(kg_{catal}·h) with a contribution of 0.57 kg alcohols/(kg_{catal}·h) and 1.02 kg liquid hydrocarbons/(kg_{catal}·h). The alcohol products in the resulting biofuels were dominated by the $C2^+$ alcohols (mainly C2−C6 alcohols) with a content of 73.55%−89.98%. The selectivity of the liquid hydrocarbons ($C5^+$) in the hydrocarbon products ranges from 60.37% to 70.94%. The synthesis biofuels also possess a higher heat value of 40.53−41.49 MJ/kg. The effects of the synthesis conditions, including temperature, pressure, and gas hourly space velocity, on the biofuel synthesis were investigated in detail. The catalyst features were characterized by inductively coupled plasma and atomic emission spectroscopy, X-ray diffraction, temperature programmed reduction, and the N_2 adsorption-desorption isotherms measurements. The present biofuel synthesis with a higher biofuel yield and a higher selectivity of liquid hydrocarbons and $C2^+$ alcohols may be a potentially useful route to produce clean biofuels and chemicals from biomass.

Key words: Biomass, Biofuel, Higher alcohol, Liquid hydrocarbon, FeCuZnAlK catalyst

I. INTRODUCTION

Biomass is a rich, environmentally friendly and renewable resource which can be used as an alternative feedstock for energy sources or chemicals in future [1, 2]. As an only renewable carbon resource, biomass can be converted from solid phase into a wide range of liquid fuels (biofuels) or chemicals such as bio-oil, bio-ethanol, bio-diesel, liquid hydrocarbons, mixed alcohols, acetic acid, and formaldehyde [3, 4]. Through biomass gasification process, various biomass can be thermochemically converted to bio-syngas, followed by catalytic conversion to biofuels [5]. This conversion route can be performed in large quantities, whose feedstocks are unstinted by types of biomass including cellulose, hemicellulose and lignin in real application.

Mixed alcohols, generally containing C1−C6 alcohols, have been researched extensively recently [6, 7]. Compared to methanol, mixed alcohols with a higher content of $C2^+$ alcohols are more attractive as gasoline additives to enhance octane values because of the lower vapor pressure, better solubility with liquid hydrocarbons and higher overall heating value [8]. In addition, mixed alcohols can be separated into various higher value-added alcoholytic chemicals [9]. Syngas conversion to ethanol or mixed alcohols has been explored using a wide range of homogeneous and heterogeneous catalysts which have been well reviewed recently [6, 10]. Currently, the commercial production of bio-ethanol has been realized through fermentation of limited sugar-containing biomass such as corn, sugarcane, wheat and sweet potatoes [11]. Biomass gasification-synthesis route could produce bio-ethanol and mixed alcohols using unlimited types of biomass resource in large quantities. Although there is a growing worldwide interest in this topic for the past decades, the efficient catalytic conversion of bio-syngas to bio-ethanol or mixed alcohols remains challenging. Significant improvements in catalysts and processing need to be achieved to make this conversion more efficient.

Some recent studies have indicated that the use of Fischer-Tropsch synthesis (FTS) technology for biomass conversion to hydrocarbons may offer a promising and carbon neutral alternative to most conventional vehicle fuels including gasoline, diesel, and kerosene [5, 12]. In principle, many process configurations for the conversion of biomass to FTS fuels are possible. The inte-

*Author to whom correspondence should be addressed. E-mail: liqx@ustc.edu.cn

grated biomass gasification-FTS (BG-FTS) process is considered as one of the most promising routes to produce the FT fuels from biomass [13]. The main process steps in the BG-FTS consist of biomass pre-treatment (grinding and drying), biomass gasification (by air or oxygen), gas cleaning, gas conditioning and FT synthesis [14]. As far as we know, no commercial process exists up to now for production of mixed alcohols and hydrocarbons from bio-syngas. The improvements in the following aspects may be required to make this conversion close to commercial attraction. (i) The biofuel yields from bio-syngas need to be further enhanced by optimizing synthesis catalysts and operating conditions. (ii) To obtain a maximum amount of long chain hydrocarbons, the selectivity toward $C5^+$ in the FTS products should be further raised by suppressing the formation of C1−C4 hydrocarbons.

In our previous work, much attention has been paid to produce bio-syngas from biomass gasification and bio-oil steam reforming in Lab or pilot plant scales [15−19]. In this work, we efficiently produce biofuels containing mixed alcohols and liquid hydrocarbons through the FTS approach using the bio-syngas from biomass gasification over FeCuZnAlK catalysts. Especially, the biofuel synthesis together with the evaluation of biofuels would be helpful to promote real application in producing biofuels and high value-added chemicals.

II. EXPERIMENTS

A. Catalyst preparation and characterization

The mixed oxide catalysts of FeCuZnAlK with a settled molar ratio were prepared by the side-by-side co-precipitation method at a constant pH (7.0±0.2) using respective metal nitrates as precursors and K_2CO_3 as a precipitator. Main preparation procedures included: (i) preparation of the respective metal nitrate solutions, (ii) preparation of the K_2CO_3 precipitator (0.75 mol/L), (iii) preparation of the precipitates by the side-by-side co-precipitation of respective metal nitrate solutions with the precipitator at 80 °C with a constant pH (7.0±0.2), (iv) after aging for 10 h at 25 °C, the precipitate was filtered and washed with the deionized water, then dried overnight in air at 110 °C, (v) the potassium promoter was added by the incipient wetness pore-filling technique, (vi) the precipitate was calcined at 450 °C for 4 h in air to obtain the corresponding mixed oxide catalysts, (vii) the mixed oxide catalysts were finally crushed into 250−380 μm for the biofuel synthesis.

The content of the metal oxides in the catalysts were measured by inductively coupled plasma and atomic emission spectroscopy (ICP/AES, Atom scan Advantage of Thermo Jarrell Ash Corporation, USA). The Brunauer-Emmett-Teller (BET) surface area and pore volume was determined by the N_2 physisorption at −196 °C using a COULTER SA 3100 analyzer. X-ray diffraction (XRD) patterns from the fresh and reduced catalysts were measured by an X'pert Pro Philips diffractrometer, using a Cu Kα radiation (λ=154.1841 pm). The measurement conditions were in the range of 2θ=20°−80°, step counting time 5 s, and step size 0.017° at 298 K. The temperature programmed reduction (TPR) tests were performed to study the reduction features of the catalysts. Before the run, the sample was treated in flowing argon (30 mL/min) for 1 h. Subsequently, the reducing gas, a mixture of 10%H_2 diluted by argon, was switched on at a flow rate of 40 mL/min, and the temperature of the sample was increased from 100 °C to 750 °C at a constant rate of 10 °C/min. The amount of hydrogen consumption was measured by a thermal conductivity detector.

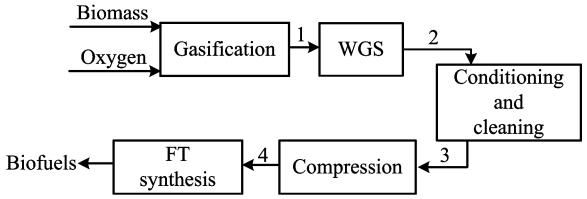

FIG. 1 Scheme of the basic process steps for converting biomass to biofuels.

B. Feedstock for the biofuel synthesis

In this work, the bio-syngas derived from biomass gasification was used for the biofuel synthesis (this bio-syngas was provided by Hefei Tianyan Green Energy Development Co., Ltd, Hefei, China). The main composition of the bio-syngas is H_2 62.80%, CO 30.89%, CO_2 2.96%, N_2 1.75%, CH_4 1.20%, and others 0.40% in vol %, respectively. Figure 1 presents a scheme of the basic process steps for converting biomass to biofuels. Rice husks were first gasified in the gasifier with pressurized oxygen (1.5−3.0 MPa) at 1000−1300 °C [20]. Before the raw bio-syngas was compressed and fed into the FT reactor, it must be adjusted via the water gas shift (WGS) reaction, cleaning (purging poisons of H_2S, COS (carbonyl sulphide), *etc.*) and conditioning (CO_2 removal) process steps to make it suitable for the catalytic FT synthesis. The main composition of the bio-syngas through several operation processes is shown in Table I.

C. Reaction system for the biofuel synthesis

The performance of the biofuel synthesis from the bio-syngas over the FeCuZnAlK catalysts was evaluated in a fixed-bed continuous-flow reactor using an online gas chromatograph (GC) detection system. Usually, 1.0 g catalyst, diluted with 2.0 mL Pyrex beads,

DOI:10.1088/1674-0068/24/06/745-752

TABLE I Main composition (in unit of %) of the bio-syngas in real operation processes.

Compositions	Step-1[a]	Step-2	Step-3	Step-4
N_2	1.48	1.22	1.75	1.75
H_2	33.25	44.25	62.80	62.80
CO	46.21	21.35	30.89	30.89
CO_2	17.63	32.07	2.96	2.96
H_2S+COS[b]	0.08	0.04	–	–
CH_4	1.00	0.80	1.20	1.20
Others[c]	0.35	0.27	0.40	0.40
Pressure/MPa	0.55/1.05	0.45/0.95	0.35/0.85	7.0

[a] Steps 1−4 stand for the bio-syngas preparation processes described in Fig.1.
[b] Carbonyl sulphide (COS).
[c] Containing Ar, C2−C4 gasous hydrocarbons.

was used for each test. Before the synthesis reactions, the catalyst was pre-reduced in situ by a flowing 10%H_2/Ar mixture with a stepwise reduction procedure up to 450 °C for 20 h. Then, the syngas was fed into the reactor for the biofuel synthesis under a setup synthesis condition. Products were quantitatively online analyzed by two gas chromatographs systems every 30−60 min. The gases of H_2, CO, N_2, and CO_2 were detected by GC1 (Model: SP6890, column: TDX-01) with a thermal conductivity detector (TCD), using ultrahigh purity argon (99.999%) as carrier gas and gas hydrocarbons were detected by GC2 (Model: SP6890, column: PoraparkQ-S, USA) with a flame ionization detector (FID). The condensable organic vapors (mainly mixed alcohols and liquid hydrocarbons) were cooled into a liquid tank and then were detected by GC3 (Model: SP6890, column: SE30 capillary column) with a FID. The performance of the biofuel synthesis was evaluated by carbon conversion, space time yield of total biofuels (STY(bio.)), yield of mixed alcohols (STY(alc.)) and liquid hydrocarbons (STY (LHC)), selectivity of alcohols ($S_{\rm alc}$) and hydrocarbons ($S_{\rm HCs}$), and heat value (HV), according to the following equations [21, 22]:

$$\mathrm{C}\% = \frac{x_{\rm inCO} - x_{\rm outCO}}{x_{\rm inCO}} \times 100\% \quad (1)$$

where $x_{\rm inCO}$ and $x_{\rm outCO}$ are the carbon moles of $CO_{\rm in}$, $CO_{\rm out}$, respectively. The conversion of CO+CO_2 was defined as:

$$\mathrm{C}_{\rm CO+CO_2}\% = \frac{x_{\rm inCO+CO_2} - x_{\rm outCO+CO_2}}{x_{\rm inCO+CO_2}} \times 100\% \quad (2)$$

$$\mathrm{STY(alc.)} = \frac{M_{\rm alc.}}{M_{\rm catal}t} \quad (3)$$

$$\mathrm{STY(LHC)} = \frac{M_{\rm liquid}}{M_{\rm catal}t} \quad (4)$$

$$\mathrm{STY(bio.)} = \mathrm{STY(alc.)} + \mathrm{STY(LHC)} \quad (5)$$

$$S_{\rm alc.} = \frac{M_{\rm alc.}}{M_{\rm all}} \times 100\% \quad (6)$$

TABLE II Performance of the biofuel synthesis using the bio-syngas over the $Fe_{1.5}Cu_1Zn_1Al_1K_{0.117}$ catalyst (T in °C, P in MPa, GHSV in 10^4 h^{-1}, and HV in MJ/kg).

Condition			C/%	STY/(g/(kg_{catal}· h))			HV
T	P	GHSV		Alcohol	LHC	Biofuel	
260	5.0	1	31.50	79.35	178.90	258.25	41.31
280	5.0	1	62.00	184.69	334.70	519.39	40.58
300	5.0	1	94.30	308.01	710.00	1018.01	41.49
330	5.0	1	90.39	286.99	581.73	868.72	41.02
300	5.0	2	78.38	475.00	892.20	1367.20	40.80
300	7.0	2	88.40	570.10	1022.13	1592.23	40.53

$$S_{\rm HC_s} = \frac{M_{\rm liquid}}{M_{\rm all}} \times 100\% \quad (7)$$

where $x_{\rm inCO+CO_2}$ and $x_{\rm outCO+CO_2}$ are the carbon moles of CO+$CO_{2\rm in}$ and CO+$CO_{2\rm out}$, respectively; and $M_{\rm alc.}$, $M_{\rm catal}$, $M_{\rm all}$, and $M_{\rm liquid}$ are weight of alcohols, catalyst, liquid hydrocarbons, and all liquid organic compounds, respectively. In addition, the heat values of biofuels containing mixed alcohols and liquid hydrocarbons were measured by an XRY-1B Microcomputer oxygen bomb calorimeter.

III. RESULTS AND DISCUSSION

A. Synthesis of biofuels from bio-syngas

In present work, the biofuel synthesis was carried out using the bio-syngas obtained from biomass gasification and the $Fe_{1.5}Cu_1Zn_1Al_1K_{0.117}$ catalyst. According to the catalyst screening tests, a suitable composition of the FeCuZnAlK catalysts for the biofuel synthesis contains 25%−45% Fe_2O_3, 20%−30% CuO, 20%−30% ZnO, 5%−20% Al_2O_3 and 1%−5% K_2O, respectively. In particular, the $Fe_{1.5}Cu_1Zn_1Al_1K_{0.117}$ catalyst with an atomic ratio of Fe:Cu:Zn:Al:K=1.5:1:1:1:0.117 showed a higher catalytic activity in the biofuel synthesis with a higher selectivity toward $C2^+$-alcohols and $C5^+$-liquid hydrocarbons. Thus, much attention in this work has been paid to the production of biofuels from the bio-syngas over the $Fe_{1.5}Cu_1Zn_1Al_1K_{0.117}$ catalyst. Table II shows the performance of the biofuel synthesis using the bio-syngas over the $Fe_{1.5}Cu_1Zn_1Al_1K_{0.117}$ catalyst under the synthesis conditions: T=260−330 °C, P=5.0−7.0 MPa, and gas hourly space velocity (GHSV)=10^4−2×10^4 h^{-1}. The maximum STY (biofuels) of total mixed biofuels was about 1.59 kg biofuels/(kg_{catal}·h) with a contribution of 0.57 kg alcohols/(kg_{catal}·h) and 1.02 kg liquid hydrocarbons/(kg_{catal}·h) within our investigated range. In addition, present biofuels have higher heat values of 40−42 MJ/kg, which are close to those of petroleum-derived gasoline fuels (46 MJ/kg) and diesel fuels (43 MJ/kg) [23].

DOI:10.1088/1674-0068/24/06/745-752

TABLE III Selectivity and distribution of alcohols in the synthesis products using the bio-syngas over the $Fe_{1.5}Cu_1Zn_1Al_1K_{0.117}$ catalyst.

Condition			S_{alc}/%	Alcohol distribution/%						
T/°C	P/MPa	GHSV/10^4 h^{-1}		C1	C2	C3	C4	C5	C6	$C2^+$
260	5.0	1	30.13	26.45	39.79	16.78	12.44	3.55	0.99	73.55
280	5.0	1	34.86	15.03	60.30	15.64	6.50	2.01	0.52	84.97
300	5.0	1	30.00	13.62	61.63	15.16	6.90	2.10	0.59	86.38
330	5.0	1	32.24	10.02	70.11	13.91	4.30	1.44	0.22	89.98
300	5.0	2	34.04	12.54	62.09	15.06	6.67	2.72	0.92	87.46
300	7.0	2	34.80	13.68	63.88	14.63	5.50	1.88	0.43	86.32

Temperature is one of the most critical reaction parameters in the biofuel synthesis, which significantly influences the rate of kinetically controlled synthesis reactions. As shown in Table II, the carbon conversion significantly increases from 31.50% to 94.30% with a rising temperature from 260 °C to 300 °C, but decreases as temperature exceeds 300 °C. A similar trend is also observed for the biofuel yield, giving a maximum value around 300 °C. In the lower temperature region, increasing temperature is conducive to promote the CO and CO_2 hydrogenation, because the formation of the important intermediates (*e.g.*, alkyls and formyl species) via the dissociative adsorption of CO, CO_2, and H_2 was enhanced [24]. However, another important characteristic of the biofuel synthesis is the unavoidable production of a large amount of heat from the highly exothermic synthesis reactions, and exorbitant temperature will decrease the synthesis reaction rates and shorten the catalyst lifetime [25, 26]. Consequently, to maximize the biofuel yield, an appropriate temperature should be controlled near 300 °C when the bio-syngas and the $Fe_{1.5}Cu_1Zn_1Al_1K_{0.117}$ catalyst were employed. On the other hand, pressure and GHSV are another two important factors that affect the biofuel synthesis. The carbon conversion and the STY(bio.) ascend as pressure increases (Table II). Increasing pressure favor to increase the equilibrium concentration of the alcohols and hydrocarbons in the biofuel synthesis process because the synthesis reactions involve in a decrease in the number of molecules (*e.g.*, from 6 to 2 in the CO hydrogenation to ethanol: $2CO+4H_2 \rightarrow C_2H_5OH+H_2O$). It was also observed that the biofuel yield increased and the carbon conversion decreased with increasing GHSV. The negative impact of GHSV on the carbon conversion may result from shortening residual time in the catalyst bed. The positive impact on the fuel yield may arise from the increase of the turnover frequency of the synthesis products with increasing GHSV [27].

Tables III and IV show the selectivity and distribution of the alcohols and hydrocarbons in the resulting biofuels from the bio-syngas over the $Fe_{1.5}Cu_1Zn_1Al_1K_{0.117}$ catalyst. The selectivity towards the alcohols S_{alc} (mainly from C1 to C6 alcohols) ranges from 30.0% to 34.86%. The selectivity of hydrocarbons

TABLE IV Selectivity and distribution of hydrocarbons in the synthesis products using the bio-syngas over the $Fe_{1.5}Cu_1Zn_1Al_1K_{0.117}$ catalyst (T in °C, P in MPa, and GHSV in 10^4 h^{-1}).

Conditions			S_{HCs}/%	Hydrocarbons distribution/%				
T	P	GHSV		C1	C2	C3	C4	$C5^+$
260	5.0	1	65.79	8.90	7.61	8.68	3.87	70.94
280	5.0	1	62.32	10.33	7.74	8.89	4.60	68.44
300	5.0	1	69.06	11.40	7.57	8.56	4.72	67.75
330	5.0	1	65.90	12.77	7.84	8.75	5.32	65.32
300	5.0	2	63.89	15.20	8.65	9.59	6.19	60.37
300	7.0	2	61.68	11.95	7.12	8.07	4.99	67.87

S_{HCs} is in the region of 61.68%−69.06% under our investigated conditions. The alcohol products in the resulting biofuels were dominated by the $C2^+$ alcohols with content of 73.55%−89.98%. The selectivity of the liquid hydrocarbons ($C5^+$) in the hydrocarbon products ranges from 60.37% to 70.94%. Apart from the alcohol and hydrocarbon products, only a small amount of other compounds including aldehydes, ketones, esters, and ethers were also detected, whose content is 0.94%−4.08% in the liquid organic products. The above results indicate that the $Fe_{1.5}Cu_1Zn_1Al_1K_{0.117}$ catalyst favors to produce the liquid hydrocarbons and higher alcohols (C2−C6 alcohols).

Moreover, the catalytic stability in the biofuel synthesis process was tested by measuring the CO conversion, conversion of $CO+CO_2$, yields of alcohols and liquid hydrocarbons as a function of time on stream. The activity increases initially until it reaches the maximum, and then it decreases very slowly with increasing time-on-stream (Fig.2). The carbon conversion and the yields of biofuels reach the maximum at about 4−5 h of time on stream. Subsequently the catalytic activity lasts for more than 50 h. A long-term (100 h) reaction test led to about 8%−10% reduction in the biofuel synthesis activity compared to the maximum values. The slow catalyst inactivation observed in the biofuel synthesis process was mainly caused by the carbon deposition in present biofuels.

DOI:10.1088/1674-0068/24/06/745-752

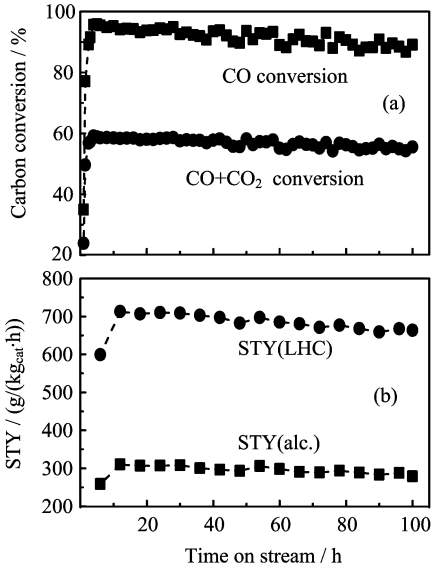

FIG. 2 Stability of the $Fe_{1.5}Cu_1Zn_1Al_1K_{0.117}$ catalyst in the biofuel synthesis using the bio-syngas. (a) Conversion of CO and ($CO+CO_2$). (b) STY of alcohols and LHC. Synthesis conditions: T=300 °C, P=5.0 MPa and GHSV=10^4 h^{-1}.

B. Characterization of synthesis catalysts

The synthesis catalyst of $Fe_{1.5}Cu_1Zn_1Al_1K_{0.117}$ was characterized by XRD, TPR, and BET techniques. The fresh catalyst before the reduction presents a BET surface area (S_{BET}) of 60.84 m^2/g and a total pore volume (V_p) of 0.31 cm^3/g, respectively. After the reduction in a flowing 10% H_2/Ar mixture for 20 h, S_{BET} slightly decreases to 55.73 m^2/g and V_p (0.36 cm^3/g) changes a little. Figure 3 shows the XRD patterns from two different samples, including the fresh $Fe_{1.5}Cu_1Zn_1Al_1K_{0.117}$ catalyst calcined at 450 °C for 4 h in air and the reduced one (reduction condition: a stepwise reduction procedure up to 450 °C for 20 h in a flowing 10% H_2/Ar mixture). For the fresh catalyst (Fig.3(a)), the main characteristic peaks are identified as the diffractions of CuO, Fe_2O_3 or Fe_2ZnO_4 metallic oxides. The XRD patterns appear as a series of dispersive profiles, suggesting that the metallic oxides may present in a relative dispersed state in the fresh catalyst. After the reducing treatment (Fig.3(b)), a series of new peaks were observed, corresponding to the metallic phases of Fe (2θ=44.70°, 65.05°) and Cu (2θ=42.69°, 49.75°, and 72.82°) according to PDF-06-0696 and 04-0836 cards (International Centre for Diffraction Data (ICDD), 2002). In addition, the mean particle sizes of the specific metals or oxides were calculated by the Scherrer equation [28]. The mean particle diameters of CuO and Fe_2O_3 in the fresh catalyst are about 7.73 and 6.62 nm respectively, and slightly increase to 9.26 nm for the Cu species, 10.52 nm for the Fe species and 7.35 nm for the Fe_3O_4 species after the reduction treatment.

Figure 4 (a)−(c) shows the TPR profiles of onefold

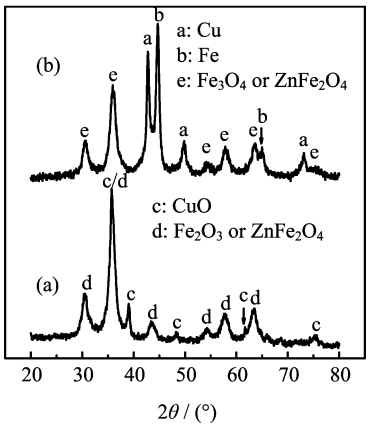

FIG. 3 XRD spectra for (a) the fresh catalyst and (b) the reduced catalyst of $Fe_{1.5}Cu_1Zn_1Al_1K_{0.117}$.

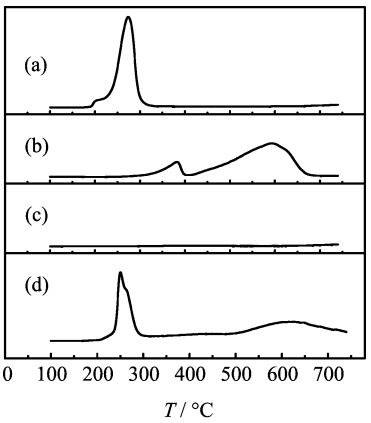

FIG. 4 H_2-TPR profiles with H_2 consumption as a function of temperature (a) CuO, (b) Fe_2O_3, (c) ZnO, and (d) $Fe_{1.5}Cu_1Zn_1Al_1K_{0.117}$.

metal oxide (CuO, Fe_2O_3, ZnO). The TPR pattern of CuO sample displays a strong reduction peak near 274 °C in the temperature region of 190−330 °C. The TPR profile of Fe_2O_3 presents two reduction peaks, *i.e.*, a weaker peak near 382 °C and a stronger asymmetric peak at about 593 °C, which are attributed to the reduction from Fe_2O_3 to Fe_3O_4 and the stepwise reduction of Fe_3O_4→FeO→Fe (metallic iron), respectively. No distinct reduction peak is observed from ZnO sample, which suggests ZnO was hardly reducible under the investigated conditions. As is shown in Fig.4(d), three reduction peak profiles appear in the TPR pattern of the $Fe_{1.5}Cu_1Zn_1Al_1K_{0.117}$ catalyst sample. The first peak profile in the low temperature range of 210−300 °C has a distinct reduction peak near 250 °C which is assigned to the reduction of dispersed CuO. There is another weaker shoulder peak near 265 °C which is assigned to the CuO reduction in the bulk [29, 30]. The overall CuO reduction profile obviously shifts to the lower temperature and the reduction peak corresponding to the dispersed CuO reduction (near 250 °C) becomes

DOI:10.1088/1674-0068/24/06/745-752

predominant, compared with that of the onefold metal oxide CuO. This implies that the dispersion of CuO was enhanced in the FeCuZnAlK catalyst. The second and third peak profiles, which correspond to the stepwise reduction from Fe_2O_3 to metallic iron, become more broadening. For the Fe_2O_3 reduction in the onefold metal oxide and the FeCuZnAlK catalyst, no obvious shift was observed, indicating that there was no strong interaction of Fe_2O_3 with other components in the catalyst. In addition, the H_2 consumption for CuO and Fe_2O_3 in the $Fe_{1.5}Cu_1Zn_1Al_1K_{0.117}$ catalyst is 2.59 and 4.19 mmol/g, while the H_2 consumption for ZnO is almost zero. The level of the catalyst reduction for specific metallic of Fe and Cu was described by the ratio of r_M=[M^0]/([M^0]+[M^{x+}]) (M=Fe and Cu) on the basis of their H_2 consumption measured and the required amount for the reduction of maximum valence metal oxide to metal. The reduction degrees of Fe_2O_3 and CuO for the $Fe_{1.5}Cu_1Zn_1Al_1K_{0.117}$ catalyst are about 64.77% and 91.09%, respectively. The above results indicated that most of the metallic oxides (CuO and Fe_2O_3) in the fresh $Fe_{1.5}Cu_1Zn_1Al_1K_{0.117}$ catalyst (*i.e.*, after the calcining treatment) were reduced into the metal states (Cu, Fe) through the reduction treatment. Fe is well known as one of FT synthesis elements and plays an important role in the carbon chain-growth. The Cu species in the reduced $Fe_{1.5}Cu_1Zn_1Al_1K_{0.117}$ catalyst favor to enhance the alcohols-formation.

C. Mechanism and evaluation of biofuel synthesis

The Cu-Co-based catalysts can produce mixed alcohols using a H_2/CO ratio of 2.0−2.5, whose typical yield is 0.1−0.6 kg alcohols/(kg_{catal}·h) with a content of $C2^+$-alcohols in the alcohol products ranging from 20% to 70% [10]. In the Fischer-Tropsch synthesis, Fe-based catalysts are generally utilized to produce gasoline under a H_2/CO ratio of 0.5−2.5 with a yield of 0.47−0.94 kg liquid hydrocarbons/(kg_{catal}·h) and a content of $C5^+$-hydrocarbons in the hydrocarbon products ranging between 40% and 85% [31, 32]. As shown in Tables II−IV, the FeCuZnAlK catalyst is conducive to produce fairly high yields of alcohols and liquid hydrocarbons (LHC, $C5^+$-hydrocarbons), reaching the maximum yield of 0.57 kg alcohols/(kg_{catal}·h) and 1.02 kg LHC/(kg_{catal}·h), respectively. Thereinto, the selectivity to the $C2^+$-alcohols in the alcohols products ranges between 70% and 90%. Accordingly, present catalyst may be one of the most suitable candidates for the biofuel synthesis from the bio-syngas because this non-noble metal catalyst can efficiently produce higher alcohols and liquid hydrocarbons through the hydrogenation of CO and CO_2.

The catalyst of FeCuZnAlK employed in this work belongs to the modified FT synthesis catalyst. In the FeCuZnAlK system, Fe is well known as one of FT synthesis elements and plays an important role in the carbon chain-growth [10, 33], which leads to an increase of the selectivity towards the $C2^+$-alcohols and $C5^+$-liquid hydrocarbons. Adding the promoters of Cu and Zn to the FeCuZnAlK synthesis catalysts favors to enhance the alcohols-formation. In addition, the CO molecules adsorbed dissociatively in the CO hydrogenation reactions are responsible for hydrocarbon formation while those adsorbed associatively favor the formation of alcohols [34]. The addition of alkali metal to the synthesis catalysts may reduce the CO dissociative adsorption and increasing the associatively adsorbed CO by blocking the active sites (Fe, Cu), favoring to formation of alcohols [35]. Concerning the formation of higher alcohols over a modified Fe-based FTS catalysts through the CO hydrogenation, a generally accepted mechanism is "the CO insertion mechanism" [6, 10]. In this mechanism, adsorbed formyl species (HC=O(a)) and adsorbed alkyl species (CH_x(a)) can be first formed from the associative or dissociative adsorption of CO and H_2. Then, the adsorbed CO(a) can insert to the alkyl species CH_x(a) and form adsorbed acetyl species ($H_xC-C=O$(a)), followed by adding the H(a) species to produce ethanol. Furthermore, the adsorbed CO(a) can insert to the higher carbon-numbers' alkyl species C_nH_x(a) which are generated through the chain-growth step and form adsorbed intermediate species ($C_nH_x-C=O$(a)), followed by adding the H(a) species to produce the $C3^+$ alcohols. On the other hand, the formation of hydrocarbons through the hydrogenation of CO over modified Fe-based FTS catalysts is recognized as "$-CH_2$-group polymerization reactions" with the following steps including (i) CO adsorption on the catalyst surface, (ii) chain initiation through CO dissociation followed by hydrogenation, (iii) chain growth via insertion of additional CO molecules followed by hydrogenation, (iv) chain termination, and (v) product desorption from the catalyst surface [36, 37]. The selectivities and distributions of various hydrocarbons or alcohols could be described by the Anderson-Shulz-Flory (ASF) equation [38]:

$$\ln \frac{W_n}{n} = n \ln \alpha + \ln \frac{(1-\alpha)^2}{\alpha} \tag{8}$$

where W_n is the weight percentage of a product containing n carbon atoms and α is the chain growth probability. As shown in Fig.5, the product distributions are consistent with the Schulz-Flory (SF) equation very well, except that methane and methanol show an obvious deviation. α for hydrocarbons and alcohols, derived from the slope of the SF plots, is about 0.764±0.004 and 0.247±0.014, respectively. The different α values may suggest that the formation of hydrocarbons and alcohols take place in different active sites. The hydrocarbons could be produced on the iron sites, but the alcohols could be produced near the copper sites.

Finally, Table V shows a comparison and evaluation for four biofuels, *i.e.*, present biofuels, bio-ethanol, bio-diesel, and bio-oil, according to different biomass

DOI:10.1088/1674-0068/24/06/745-752

TABLE V Comparison of the selected biofuels derived from different processes.

Bio-fuels	Bio-fuel[a] (this work)	Bio-ethanol [11, 40]	Bio-diesel [4, 39, 41−43]	Bio-oil [44, 45]
Raw materials	Various biomass	Sugars-containing crops	Vegetable or animal fat & oil	Various biomass
Processes	Fuel synthesis via bio-syngas	Fermentation	Transesterification reaction	Fast pyrolysis
Typical-conditions	Gasification: 1200 °C, 2 MPa, Synthesis: 300 °C, 5 MPa	Fermentation: 30−38 °C	Transesterification: 25−65 °C	Pyrolysis 450−600 °C
Yield	0.13−0.20 t fuel /(t biomass)	0.25 t EtOH /(t dry sugar cane)	0.42 t bio-diesel /(t rapeseed)	0.5−0.7 t bio-oil/(t biomass)
Cost	460−590 US$/(t bio-fuel)	290−370 US$/ (t EtOH) in Brazil	390−480 US$/(t bio -diesel) for waste grease	115−150 US$/ (t bio-oil)
Main feature	Mixed fuels with 70%−90% C_2^+ alcohols and 60%−70% LHC, HV=40−42 MJ/kg	Ethanol, HV=26.7 MJ/kg	Fatty acid mono alkyl ester, HV=32−40.5 MJ/kg	Mixed compounds, HV=16−19 MJ/kg
Main use	Transportation fuels or petrol additives, or chemicals	Gasoline additive, chemicals	Motor vehicle fuels	Combustion, production of H_2, *etc.*

[a] The cost for production of present bio-fuel in China was estimated by the following items. Cost of straw: 200 RMB/t. Cost of catalyst: 70−120 RMB/Kg. Cost of water: 3 RMB/t. Cost of power: 0.7 RMB/KWh. Cost of CO_2 separating and saving: 300 RMB/(t CO_2). Cost of bio-syngas preparation: 2270−2940 RMB/(t bio-fuel). Cost of fuel synthesis: 870−1080 RMB/(t bio-fuel).

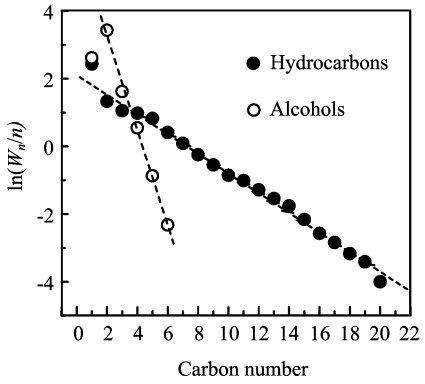

FIG. 5 Schulz-Flory plots of hydrocarbons and alcohols for the biofuel synthesis using the bio-syngas at T=300 °C, P=5.0 MPa and GHSV=10^4 h^{-1} over the $Fe_{1.5}Cu_1Zn_1Al_1K_{0.117}$.

raw materials and conversion processes. So far, only production of bio-ethanol and bio-diesel has been well-developed and commercialized [4]. However, both bio-ethanol and bio-diesel are derived from the selected and limited biomass resources. Bio-ethanol is currently produced by the fermentation of sugars-containing crops (*e.g.*, corn, sugarcane, wheat). Bio-diesel is produced by the transesterification reactions mainly using vegetable seed-oil (*e.g.*, soy bean oil, rapeseed oil, palm oil) or animal fat and oil. In viewpoint of biomass resources, the biofuels from the bio-syngas, is unstinted by the feedstocks of biomass (*e.g.*, various biomass including cellulose, hemicellulose, and lignin). Concerning the fuel yield, the estimated yield of present bio-fuels is about 0.13−0.20 t fuels/(t biomass), which is close to the levels of bio-ethanol, but obviously lower than those of bio-diesel and bio-oil [11, 28, 39]. Furthermore, we have preliminarily estimated the production costs of present biofuels including the cost of the raw materials (biomass, catalyst, and water) and the cost of the energy consumption in the biomass gasification, gas conditioning, gas compression, and fuel synthesis processes. The estimated production cost of present biofuels is about 460−590 US$/(t fuels). In addition, present bio-fuels have higher heat values between 40.53 and 41.49 MJ/kg, which are close to those of petroleum-derived gasoline fuels (46 MJ/kg) and diesel fuels (43 MJ/kg). Present biofuels may be used as transportation fuels or petrol additives.

IV. CONCLUSION

A highly efficient synthesis of clean biofuels was carried out using the bio-syngas obtained from biomass gasification and the $Fe_{1.5}Cu_1Zn_1Al_1K_{0.117}$ catalyst. The $Fe_{1.5}Cu_1Zn_1Al_1K_{0.117}$ catalyst is one of the appropriate suitable candidates for the biofuel synthesis. Main active elements in the $Fe_{1.5}Cu_1Zn_1Al_1K_{0.117}$ catalyst are metallic Fe and Cu. The conversion of the bio-syngas over the $Fe_{1.5}Cu_1Zn_1Al_1K_{0.117}$ catalyst was operated under the moderate conditions of 280−330 °C and 5.0−7.0 MPa. The maximum biofuel yield reaches about 1.59 kg fuels/(kg_{catal}·h) with a contribution of 0.57 kg alcohols/(kg_{catal}·h) and 1.02 kg liquid hydrocarbons/(kg_{catal}·h). The catalyst of $Fe_{1.5}Cu_1Zn_1Al_1K_{0.117}$ is conducive to produce liquid

DOI:10.1088/1674-0068/24/06/745-752

hydrocarbons and high alcohols. The alcohol products in the resulting biofuels were dominated by the $C2^+$ alcohols with a content of 73.55%−89.98%. The selectivity of the liquid hydrocarbons ($C5^+$) in the hydrocarbon products ranges from 60.37% to 70.94%. The synthesis biofuels also possess a higher heat value of 40.53−41.49 MJ/kg. The comparison and preliminary evaluation among present biofuels, bio-ethanol, biodiesel, and bio-oil were also made according to biomass raw materials and conversion processes. The synthesis approach of present biofuels with a higher biofuel yield and real environmental benefits may be a potentially useful route to produce clean biofuels and chemicals from biomass in future.

V. ACKNOWLEDGMENTS

This work was supported by the National Basic Research Program of Ministry of Science and Technology of China (No.2007CB210206), the National High Tech Research and Development Program (No.2009AA05Z435), and the National Natural Science Foundation of China (No.50772107).

[1] R. M. Navarro, M. A. Pena, and J. L. G. Fierro, Chem. Rev. **107**, 3952 (2007).
[2] R. D. Cortright, R. R. Davda, and J. A. Dumesic, Nature **418**, 964 (2002).
[3] L. Petrus and M. A. Noordermeer, Green Chem. **8**, 861 (2006).
[4] S. N. Naik, V. V. Goud, P. K. Rout, and A. K. Dalai, Renew. Sust. Energ. Rev. **14**, 578 (2010).
[5] M. J. A. Tijmensen, A. P. C. Faaij, C. N. Hamelinck, and M. R. M. Hardeveld, Biomass Bioenerg **23**, 129 (2002).
[6] J. J. Spivey and A. Egbebi, Chem. Soc. Rev. **36**, 1514 (2007).
[7] P. Forzatti, E. Tronconi, and I. Pasquon, Catal. Rev. Sci. Eng. **33**, 109 (1991).
[8] S. A. Hedrick, S. S. C. Chuang, A. Pant, and A. G. Dastidar, Catal. Today **55**, 247 (2000).
[9] T. K. Ng, R. M. Busche, C. C. McDonald, and R. W. F. Hardy, Science **219**, 733 (1983).
[10] V. Subramani and S. K. Gangwal, Energy Fuels **22**, 814 (2008).
[11] M. Balat and H. Balat, Appl. Energy **86**, 2273 (2009).
[12] E. V. Steen and M. Claeys, Chem. Eng. Technol. **31**, 655 (2008).
[13] M. Balat, M. Balat, E. Kirtay, and H. Balat, Energy Conv. Manag. **50**, 3158 (2009).
[14] M. M.Yung, W. S. Jablonski, and K. A. Magrini-Bair, Energy Fuels **23**, 1874 (2009).
[15] T. Kan, J. X. Xiong, X. L. Li, T. Q. Ye, L. X. Yuan, Y. Torimoto, M. Yamamoto, and Q. X. Li, Int. J. Hydrogen Energy **35**, 518 (2010).
[16] L. X. Yuan, Y. Q. Chen, C. F. Song, T. Q. Ye, Q. X. Guo, Q. S. Zhu, Y. Torimoto, and Q. X. Li, Chem. Commun. 5215 (2008).
[17] Z. X. Wang, Y. Pan, T. Dong, X. F. Zhu, T. Kan, L. X. Yuan, Y. Torimoto, M. Sadakata, and Q. X. Li, Appl. Catal. A **320**, 24 (2007).
[18] T. Hou, L. X. Yuan, T. Q. Ye, L. Gong, J. Tu, M.Yamamoto, Y. Torimoto, and Q. X. Li, Int. J. Hydrogen Energy **34**, 9095 (2009).
[19] T. Q. Ye, L. X. Yuan, Y. Q. Chen, T. Kan, J. Tu, X. F. Zhu, Y. Torimoto, M. Yamamoto, and Q. X. Li, Catal. Lett. **127**, 323 (2009).
[20] Y. Liu, F. Chen, S. X. Zhuang, J. Wang, and R. Ma, China, Patent CN 200710190420.0. (2007).
[21] Z. X. Wang, T. Dong, L. X. Yuan,T. Kan, X. F. Zhu, Y. Torimoto, M. Sadakata, and Q. X. Li, Energy Fuels **21**, 2421 (2007).
[22] W. Ma, E. L. Kugler, and D. B. Dadyburjor, Energy Fuels **211**, 832 (2007).
[23] A. Demirbas, Energy Convers. Manag. **50**, 14 (2009).
[24] G. P. van der Laan and A. A. C. M. Beenackers, Catal. Rev. Sci. Eng. **41**, 255 (1999).
[25] M. E. Dry, Catal. Today **71**, 227 (2002).
[26] X. Huang, C. W. Curtis, and C. B. Roberts, Fuel Chem. Div. Prepr. **47**, 150 (2002).
[27] Y. Liu, B. T. Teng, X. H. Guo, Y. Li, J. Chang, L. Tian, X. Hao, Y. Wang, H. W. Xiang, Y. Y. Xu, and Y. W. Li, J. Mol. Catal. A **272**, 182 (2007).
[28] F. Y. Gong, T. Q. Ye, L. X. Yuan, T. Kan, Y. Torimoto, M. Yamamoto, and Q. X. Li, Green Chem. **11**, 2001 (2009).
[29] M. Shimokawabe, H. Asakawa, and N. Takezawa, Appl. Catal. **59**, 45 (1990).
[30] R. Zhou, T. Yu, X. Jiang, F. Chen, X. Zheng, Appl. Surf. Sci. **148**, 263 (1999).
[31] A. Y. Khodakov, W. Chu, and P. Fongarland, Chem. Rev. **107**, 1692 (2007).
[32] B. H. Davis, Ind. Eng. Chem. Res. **46**, 8938 (2007).
[33] T. Inui, T. Yamamoto, M. Inoue, H. Hara, T. Takeguchi, and J. B. Kim, Appl. Catal. A **186**, 395 (1999).
[34] X. Xu, E. B. M. Doesburg, and J. J. F. Scholten, Catal. Today **2**, 125 (1987).
[35] R. J. O'Brien, L. Xu, D. R. Milburn, Y. X. Li, K. J. Klabunde, and B. H. Davis, Top. Catal. **1**, 2 (1995).
[36] A. A. Adesina, Appl. Catal. A **138**, 345 (1996).
[37] P. M. Maitlis, R. Quyoum, H. C Long, and M. L. Turner, Appl. Catal. A **186**, 363 (1999).
[38] H. Schulz, Appl. Catal. A **186**, 3 (1999).
[39] S. P. Singh and D. Singh, Renew. Sust. Energ. Rev. **14**, 200 (2010).
[40] M. Balat, H. Balat, and C. Oz, Prog. Energy Combust. Sci. **34**, 551 (2008).
[41] E. C. Petrou and C. P. Pappis, Energy Fuels **23**, 1055 (2009).
[42] Y. C. Sharma and B. Singh, Renew. Sust. Energ. Rev. **13**, 1646 (2009).
[43] M. F. Demirbas and M. Balat, Energy Convers. Manag. **47**, 2371 (2006).
[44] S. Czernik and A. V. Bridgwater, Energy Fuels **18**, 590 (2004).
[45] X. Dong, X. L. Liang, H. Y. Li, G. D. Lin, P. Zhang, and H. B. Zhang, Catal. Today **147**, 158 (2009).

DOI:10.1088/1674-0068/24/06/745-752